On the structure of As_2Te_3 glass

2006 J. Phys.: Condens. Matter 18 6213

(http://iopscience.iop.org/0953-8984/18/27/005)

INSTITUTE OF PHYSICS PUBLISHING JOURNAL OF PHYSICS: CONDENSED MATTER

J. Phys.: Condens. Matter **18** (2006) 6213–6224 doi:10.1088/0953-8984/18/27/005

On the structure of As_2Te_3 glass

M Dongol[1], Th Gerber[2], M Hafiz[3], M Abou-Zied[1] and A F Elhady[1]

[1] Physics Department, Faculty of Science, South Valley University, Qena, Egypt
[2] Fachberich Physik, Universität Rostock, Universitätplatz 3, Rostock 18051, Germany
[3] Physics Department, Faculty of Science, Assuit University, Assuit, Egypt

Received 9 February 2006
Published 23 June 2006
Online at stacks.iop.org/JPhysCM/18/6213

Abstract

X-ray scattering has been used to investigate the structure of glassy As_2Te_3, prepared by quenching in liquid nitrogen. The result of the coherent scattered x-ray intensity proved that the medium-range order (MRO) is very weak, and this was attributed to the higher metallic nature of the glass. Analysis of the first two peaks in the curve of the total radial distribution function, $T(r)$, revealed that the short-range order (SRO) in the glassy state is different from that in the crystalline state, and that the first coordination sphere includes As–As and Te–Te bonds in addition to the As–Te bonds.

1. Introduction

Although a large number of studies have been devoted to understanding the structure of glassy As_2Te_3 [1–6], the exact atomic arrangement is still unclear. There are two prevalent models that were proposed to explain the short-range order of this compound. In the first model, the glass is considered to be made up of random, covalently bonded $AsTe_{3/2}$ pyramids units, as in As_2S_3 and As_2Se_3 glasses, arranged in a three-dimensional network, and the coordination number of arsenic and tellurium atoms are three and two, respectively [1–3]. The second model proposes that the SRO is chemically disordered and homopolar pairs of As–As and Te–Te, in addition to the hetropolar As–Te pairs, are found in the first coordination shell [4, 5]. The last two models agree in that the short-range order in the glassy state is different from that in the crystalline state. In disagreement with this model, Tverjanovich *et al* [6] concluded, from x-ray diffraction data, that a proportion of the arsenic atoms in glassy As_2Te_3 have octahedral coordination, similar to that in the crystalline state, in addition to the trigonal arrangements.

In this work we tried to collect more information concerning the SRO and MRO of this interesting compound using x-ray scattering data.

2. Experimental details

2.1. Sample preparation

The glassy sample was prepared using the conventional melt-quenching technique. A total weight of 5 g of high-purity (5N) constituent elements was sealed under a vacuum of

10^{-3} Pa into a cylindrical quartz ampoule, which was then heated in an electric furnace. The temperature was slowly raised to 1000 K and the melt kept at this temperature for 24 h. During the melting process, the ampoule was frequently agitated in order to achieve homogenous mixing. The glassy state of As_2Te_3 was produced by quenching the melt in liquid nitrogen [1]. The samples for x-ray measurements were prepared by pressing tablets of dimensions $10 \times 10 \times 0.5$ mm^3.

2.2. X-ray measurements

A horizontal goniometer with a four-slit collimation system, previously described in [7], was used to perform x-ray scattering experiments using a symmetrical transmission technique with θ–2θ control (where 2θ is the scattering angle). The x-ray radiation was Ag Kα (wavelength $\lambda = 0.559$ Å) from a rotating anode (50 kV, 180 mA) with a primary beam graphite monochromator. The intensities were measured at room temperature (approximately 20 °C) from $2\theta = 1.5°$ to 120° at 0.25° intervals, i.e. the scattering vector k (where $k = 4\pi \sin\theta/\lambda$) changed from 0.2933 to 19.4 Å^{-1}. The individual scattering curves were measured at least five times to minimize any long-term instrumental drift, and 10 000 counts at each angle were averaged.

3. Data reduction

The intensities mentioned above were corrected for background radiation, polarization of the x-ray beam reflected by the sample and monochromator, and absorption [8, 9]. The individual atomic scattering factors, $f(k)$, were taken from [10] and corrected for anomalous dispersion. The average incoherent scattering, $I_{\text{inc}}(k)$, was calculated according to [10] and multiplied by the Berit–Dirac recoil factor [9].

3.1. Scaling procedure

The main difficulty in the calculation of the radial distribution function (RDF) consists of the scaling procedure (converting the corrected scattered x-ray intensity, $I_{\text{corr}}(k)$, from arbitrary units to electron units). The scaling procedure was performed in two ways. Firstly, we applied the two traditional large-k and Krogh–Moe methods to adjust $I_{\text{corr}}(k)$ to the independent scattered intensity $[\langle f^2(k)\rangle + I_{\text{inc}}(k)]$ [11, 12]. Figures 1 and 2 show the corrected and scaled intensity, $I(k)$, using the last two methods and figures 3 and 4 show the reduced intensity function, $ki(k)$, ($i(k) = \{(I(k) - [\langle f^2(k)\rangle + I_{\text{inc}}(k)])/f_e^2$, where f_e is the electronic scattering factor). If all the corrections to the experimental data were known accurately and if the coherent and incoherent scattering factors were correct, the corrected and scaled intensity $I(k)$ will oscillates smoothly about the summation of the theoretical scattering $[\langle f^2(k)\rangle + I_{\text{inc}}(k)]$ at large k-values and $ki(k)$ oscillates about zero [13]. In our case, $I(k)$ and $ki(k)$ do not satisfy these conditions. This could arise from several sources, such as unidentified instrumental errors and imperfect correction procedures [14, 15]. Several alternative methods have been applied to perform the scaling process [15–17]. We have developed the following method.

The correlation function $\sigma(r)$ was calculated from the direct Fourier transformation of the corrected intensity, $I_{\text{corr}}(k)$, according to the following equation [18];

$$\sigma(r) = \frac{1}{2\pi^2}\int_{k_{\min}}^{k_{\max}} I_{\text{corr}}(k)\sin kr\,\mathrm{d}k. \tag{1}$$

The function $\sigma(r)$ represents the electronic density distribution in real space without the sharpening function $1/f_e^2$, which accentuates the errors of measurements, especially in the high-angle region. After calculating $\sigma(r)$, a very smoothed intensity curve, $I_{\text{smoot}}(k)$, was

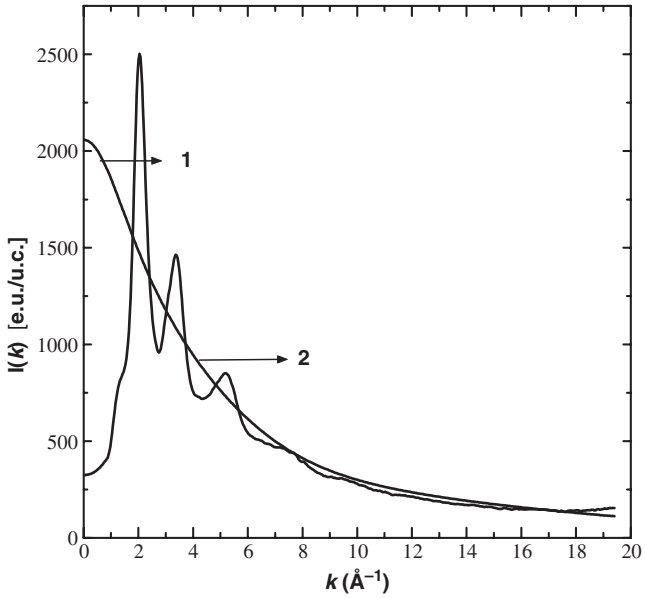

Figure 1. The k-dependent intensity distribution, $I(k)$, of glassy As_2Te_3 (curve 1) scaled to absolute units using the large-k method. Curve (2) is the theoretical scattered intensity, $[\langle f^2(k)\rangle + I_{\rm inc}(k)]$.

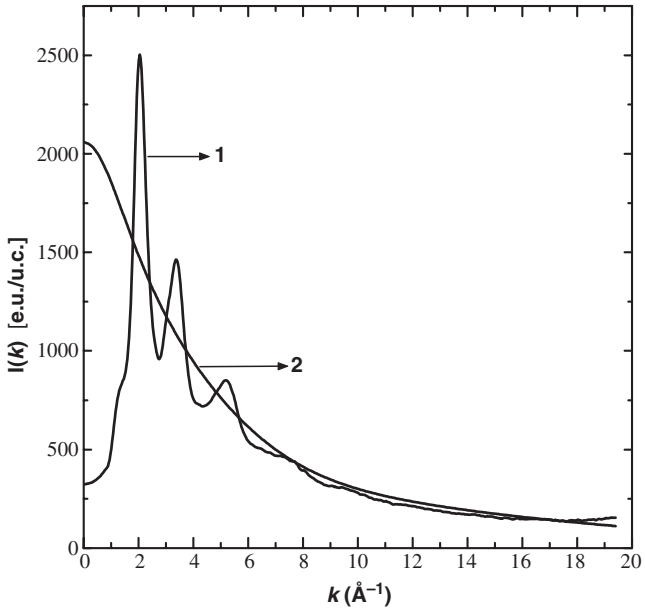

Figure 2. The k-dependent intensity distribution, $I(k)$, of glassy As_2Te_3 (curve 1) scaled to absolute units using the Krogh–Moh method. Curve (2), is the theoretical scattered intensity, $[\langle f^2(k)\rangle + I_{\rm inc}(k)]$.

produced by Fourier transformation of $\sigma(r)$ in a range of small real-space distance $r_1 \to r_2$:

$$I_{\rm smoot}(k) = 4\pi \int_{r_1}^{r_2} \sigma(r) \sin kr \, {\rm d}r. \tag{2}$$

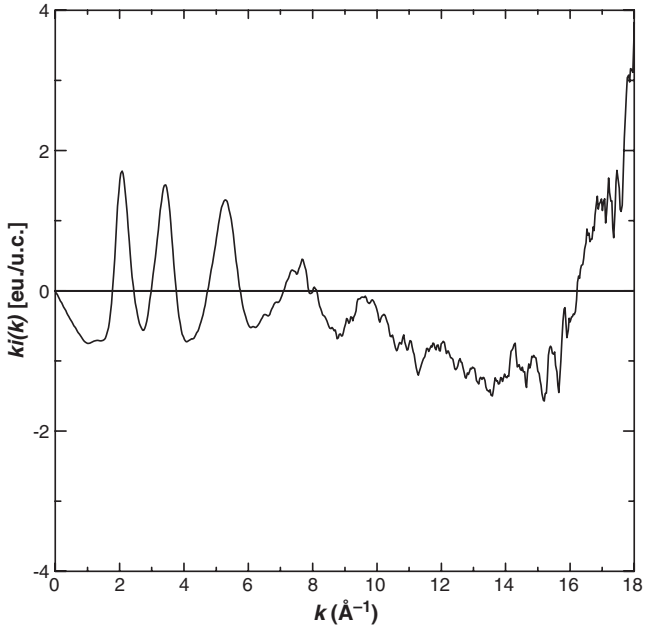

Figure 3. The reduced interference function, $ki(k)$, of the glassy As_2Te_3, calculated from the scaled intensity, $I(k)$, using the large-k method.

The range $r_1 \rightarrow r_2$ was selected carefully to make the produced $I_{\text{smoot}}(k)$ have the same features of the independent scattered intensity, especially in the high-k range ($k > 10$ Å^{-1}). Inasmuch as the first main peak in the radial distribution function corresponds to the functional form of the scattered x-ray intensity in the high-k range [19, 20], we selected the dotted region from the $\sigma(r)$ curve in figure 5 for making the Fourier transformation. Figure 6 shows the smoothed intensity curve $I_{\text{smoot}}(k)$ and $I_{\text{corr}}(k)$. The scaling process is produced by least-squares fitting of the smoothed curve $I_{\text{smoot}}(k)$ according to

$$I_{\text{smoot}}(k) = (\langle f^2(k)\rangle + I_{\text{inc}}(k)) \times F(k). \tag{3}$$

The polynomial $F(k)$ takes the form

$$F(k) = \sum_{i=0}^{n} a_i k^i \tag{4}$$

where a_i and n are the polynomial parameters and degree, respectively. Dividing through equation (3) by $(\langle f^2(k)\rangle + I_{\text{inc}}(k))$, the actual least-squares fit can be visualized. Then the corrected and scaled intensity can be written as

$$I(k) = \frac{I_{\text{corr}}(k)}{F(k)}. \tag{5}$$

The polynomial degree was selected to be low ($n \approx 2$), so that real distance correlations in $I_{\text{corr}}(k)$ are not affected. Figures 7 and 8 show $I(k)$ scaled to electron units using the new method and the produced $ki(k)$. We can notice that $I(k)$ satisfies the condition of scaling and $ki(k)$ oscillates regularly around zero in the high k-values.

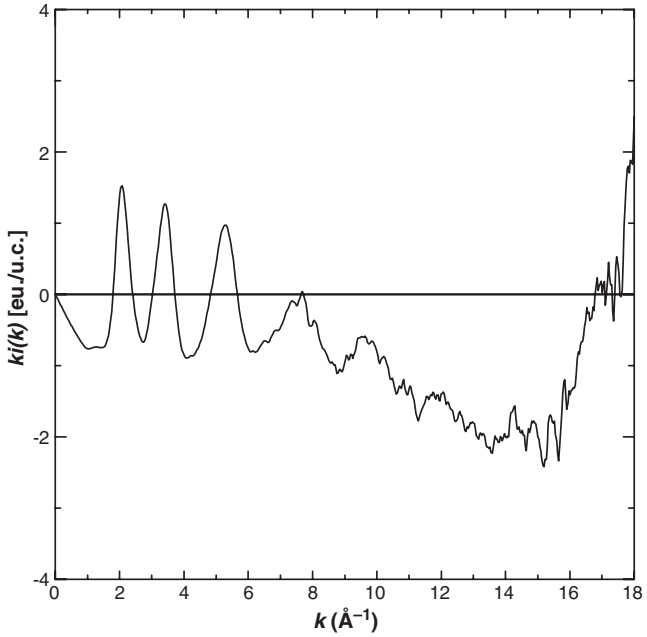

Figure 4. The reduced interference function, $ki(k)$, of the glassy As_2Te_3, calculated from the scaled intensity, $I(k)$, using the Krogh–Moe method.

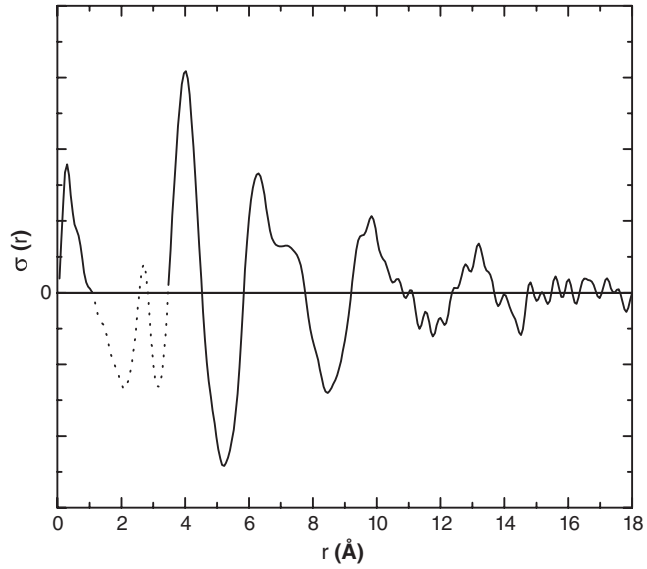

Figure 5. The correlation function, $\sigma(r)$, versus r. The dotted region is the selected range for making the Fourier transformation.

3.2. Radial distribution function

The radial distribution function (RDF), in units of e^2 Å^{-1} and in steps of 0.06 Å, was calculated from the equation [21]

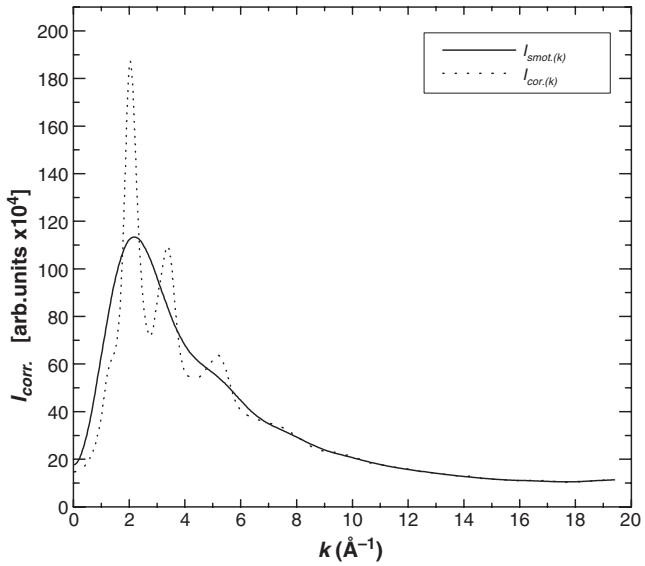

Figure 6. The corrected x-ray scattered intensity curve, I_{corr}, and the smoothed intensity curve, $I_{\mathrm{smoo.}}$, versus k for glassy As_2Te_3.

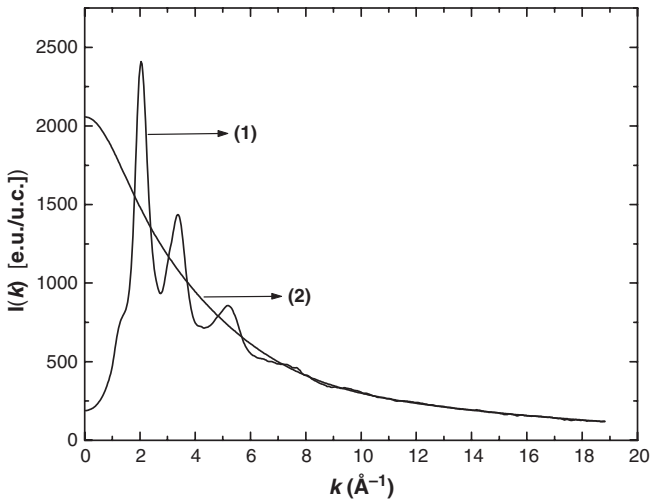

Figure 7. The k-dependent intensity distribution, $I(k)$, of glassy As_2Te_3 (curve 1). Scaled to absolute units using the new method. Curve (2) is the theoretical scattered intensity, $[\langle f^2(k)\rangle + I_{\mathrm{inc}}(k)]$.

$$\mathrm{RDF}(r) = \sum_{\mathrm{cu}} \bar{K}_m 4\pi r^2 g_m(r) = \sum_{\mathrm{cu}} \bar{K}_m 4\pi r^2 g_0 + \frac{2r}{\pi}\int_0^\infty ki(k)\sin rk\,\mathrm{d}k, \quad (6)$$

where $\bar{K}_m$ is the effective number of electrons in an atom of kind m in order to obtain the Fourier transformation; $\bar{K}_m$ was calculated using the constant effective-K approximation [21].

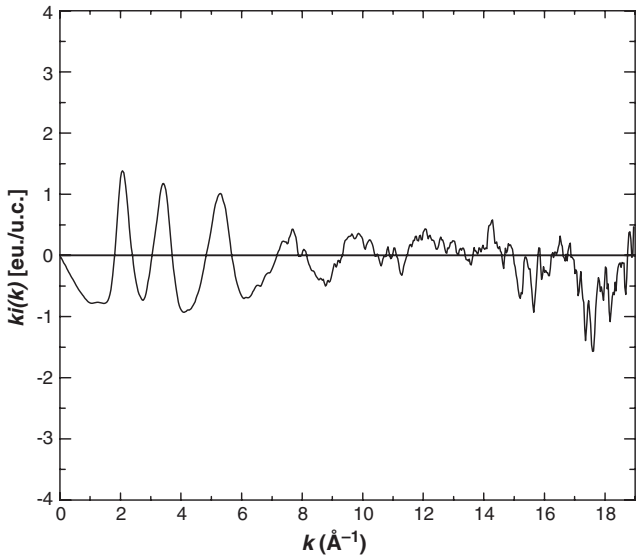

Figure 8. The reduced interference function, $ki(k)$, of glassy As_2Te_3, calculated from the scaled intensity, $I(k)$, using the new method.

$g_m(r)$ and g_0 are the local and the mean electronic density, respectively; $i(k)$ can be written as

$$i(k) = \frac{\left(\frac{I_{eu}^{\mathrm{coh}}}{N} - \langle f^2(k)\rangle\right)}{f_e^2} \tag{7}$$

where $\frac{I_{eu}^{\mathrm{coh}}}{N} (= I(k) - I_{\mathrm{inc}}(k))$ is the total coherent scattered x-ray intensity in electron units per composition unit (cu).

The average electron density around any atom in a spherical shell between radii r_1 and r_2 is given by the area, A, of a peak in RDF(r) extended from r_1 to r_2 according to

$$A = \int_{r_1}^{r_2} \mathrm{RDF}(r)\,\mathrm{d}r. \tag{8}$$

On the other hand, A is related to the partial coordination number N_{ij} expressing the average number of n atoms around an atom of kind m [22]:

$$A = \sum_{\mathrm{cu}} \bar{K}_m \bar{K}_n N_{mn}. \tag{9}$$

The function that we will use in the determination of the short-range order parameters (interatomic distances and coordination numbers) is the total correlation distribution function, $T(r)$:

$$T(r) = \frac{\mathrm{RDF}(r)}{r} = \sum_{\mathrm{cu}} \bar{K}_m 4\pi r g_0 + \frac{2}{\pi}\int_0^\infty ki(k)\sin rk\,\mathrm{d}k. \tag{10}$$

The advantage of using $T(r)$ is that the instrumental resolution enters as a symmetric function, and hence the peaks can be defined with more precision [23, 24].

4. Results and discussion

Figure 9 shows the intensity curve, I_{eu}^{coh}/N (curve 1), the theoretical coherent intensity, $\langle f^2(k)\rangle$ (curve 2) and the theoretical incoherent intensity, $I_{\mathrm{inc}}(k)$ (curve 3). It is noticed that $I_{\mathrm{inc}}(k)$ is

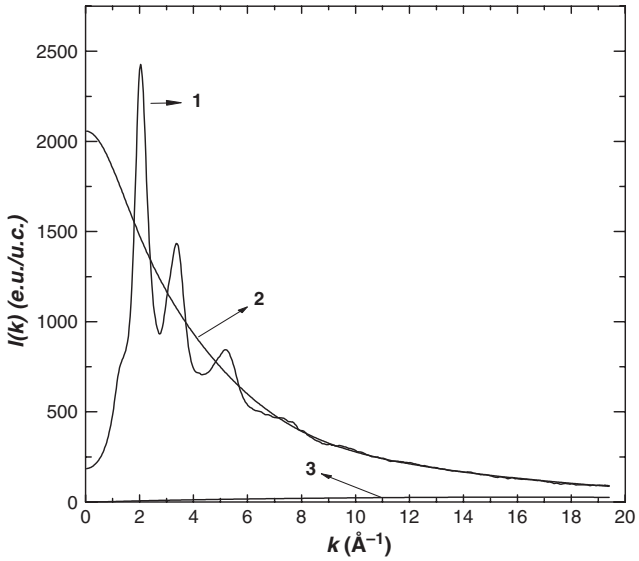

Figure 9. K-dependent coherent scattered x-ray intensity in electron units per unit of composition $\frac{I_{eu}^{\text{coh}}}{N}$ curve (1), the theoretical coherent intensity $\langle f^2(k)\rangle$ curve (2), and the theoretical incoherent intensity $I_{\text{inc}}(k)$ curve (3), for the glassy As_2Te_3 sample.

very much less than $\langle f^2(k)\rangle$, and this is expected for the heavy elements. I_{eu}^{coh}/N curve is characterized by three remarkable peaks at $k_1 = 2.04$ Å^{-1}, $k_2 = 3.36$ Å^{-1} and $k_3 = 5.21$ Å^{-1}. We can also notice a shoulder located at about 1.25 Å^{-1} and lying in the range where the first sharp diffraction peak (FSDP) appears in chalcogenide glasses [25]. This shoulder gives evidence for the existence of weak medium-range order (MRO) in the glassy As_2Te_3 sample. According to Vaipolin *et al* and Mori *et al* [26, 27], there is a proportionality between the intensity of the FSDP in $As_2S(Se, Te)_3$ glasses and the intensity of the interlayer peak in corresponding crystals. The peak intensity in the glasses and the crystals decreases in the sequence As_2S_3, As_2Se_3, and As_2Te_3. The intensity decrease in heavier atomic systems can be related to an increase in metallic nature, which reduces the distinction between intra-layer and inter-layer bonds [28].

To obtain information regarding the short-range order (SRO), the total radial distribution function, $T(r)$, was fitted using a sum of Gaussian functions,

$$T(r) = \sum_s a_i \exp\left[-\left(\frac{r - r_i}{2u_i}\right)^2\right], \tag{11}$$

where r_i and u_i represent the position and the half-width at half-height of the ith peak, respectively. The amplitude a_i is related to the peak area A_i (equation (8)) by:

$$a_i = \frac{A_i}{2u_i r_i \sqrt{\pi}}. \tag{12}$$

Gaussian fitting of the first two peaks of $T(r)$ in the range 0.0–4.5 Å are shown in figure 10. The fitting parameters shown in table 1 suggest that, in the As_2Te_3, the SRO in the glassy state is different from that in the crystalline state. The crystalline structure of As_2Te_3 consists of zigzag chains along the b axis in which the arsenic atoms octahedrally and trigonally bond to the tellurium atoms [29]. The average values of r_1 and A_1 in the crystalline state, calculated

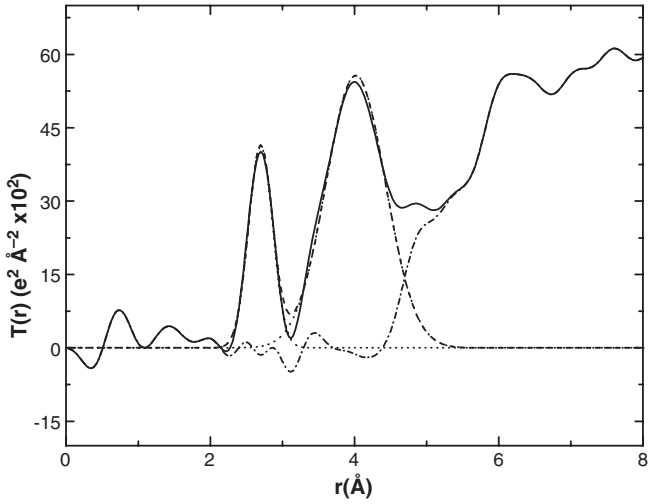

Figure 10. Fit of two nearest-neighbour shells to the total correlation function, $T(r)$, for glassy As_2Te_3. Solid line: data; dotted line: fitted peaks; dashed line: sum of fitted peaks; chain-dashed line: residual.

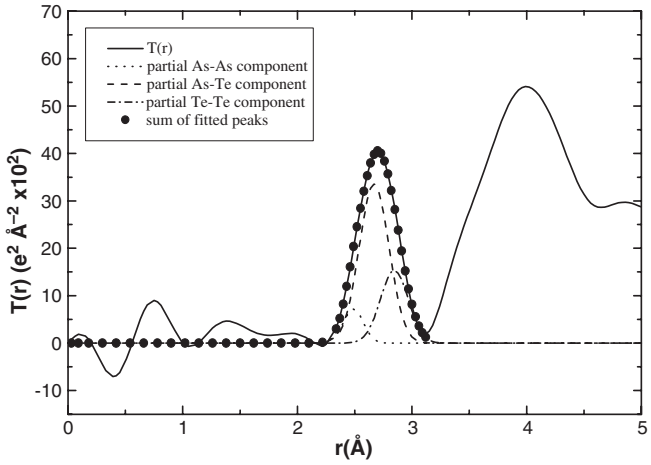

Figure 11. Decomposition of the first $T(r)$ peak into three peaks due to As–As, As–Te and Te–Te pairs for glassy As_2Te_3.

Table 1. The parameters of the two nearest-neighbour coordination shells in glassy As_2Te_3 sample.

Peak No. i	Position r_i (Å)	Mean square vibration amplitude $\langle u_i^2 \rangle$ (Å^2)	Area A_i (e^2)
1	2.68 ± 0.02	0.02	$4\,750 \pm 40$
2	4.0 ± 0.04	0.08	$23\,762 \pm 85$

according to [30], equal 2.84 Å and 7207.2 e^2, respectively. Therefore, the crystalline structure has a longer mean interatomic distance and a larger area than that in the glassy state.

In an early x-ray diffraction study of the glassy As_2Te_3 prepared by *quenching in liquid nitrogen* [1], it was already claimed that the coordination numbers of the arsenic and tellurium atoms are three and two, respectively. The structure of the As_2Te_3 glass is considered to be made up of random covalently bonded $AsTe_{3/2}$ pyramids, as in glassy As_2S_3. So, we calculated the area A_1 under the first peak, applying the chemically ordered network model (CONM) [31]. If we considered that the glassy As_2Te_3 is chemically ordered, the heteropolar As–Te bonds predominate and the atoms interact according to the 8-N [32], then equation (8) takes the following form:

$$A_1^{\mathrm{CON}} = 2C_{\mathrm{As}}\bar{K}_{\mathrm{As}}\bar{K}_{\mathrm{Te}}N_{\mathrm{As-Te}}. \tag{13}$$

The calculated area, A_1^{CON}, of 4118.4 e^2 is smaller than the experimental area of 4750 e^2. On the other hand, Cervinka *et al* concluded the same result by calculating the position of the second peak in the RDF curve, considering that the SRO consists of only $AsTe_{3/2}$ units [4]. These results indicate that the CONM is not suitable for describing the structure of glassy As_2Te_3. This conclusion was foreshadowed by neutron diffraction on liquid As_2Te_3 [30] and by electron diffraction on As_2Te_3 films [33].

Kameda *et al* [34] confirmed, using the time of flight (TOF) neutron diffraction procedure, that the first coordination shell in *liquid* As_2Te_3 involves three atomic pairs, e.g. As–Te, As–As and Te–Te. Then, considering that the random covalent network model (RCNM) [31] is suitable for interpreting the SRO of our As_2Te_3 glassy sample, $T(r)$ was fitted in the range of the first peak using the three-shell mode, corresponding to the formation of As–As, As–Te and Te–Te bonds. From equation (8), the area of subpeak A_{n-m} is connected with the partial coordination numbers N_{n-m}:

$$A_{n-m} = C_n\bar{K}_n\bar{K}_mN_{n-m}. \tag{14}$$

The total coordination number N_n of atom n can be obtained from the sum of partial coordination numbers, such as [35]

$$N_{\mathrm{Te}} = N_{\mathrm{Te-As}}(\equiv (C_{\mathrm{As}}/C_{\mathrm{Te}}) \times N_{\mathrm{As-Te}}) + N_{\mathrm{Te-Te}}. \tag{15}$$

The fitting parameters and a comparison with representative results from the literature are shown in table 2. The value of the total coordination number of arsenic atoms, N_{As}, was equal to 2.95, which satisfies 8-N rule. On the other hand, the total coordination number of Te atoms ($N_{\mathrm{Te}} = 2.33$) exceeds two, as in liquid Te with metallic character, as reported by Usuki *et al* [35]. This model explains the higher electrical conductivity of glassy As_2Te_3 ($=5 \times 10^{-5}\ \Omega^{-1}\ \mathrm{cm}^{-1}$) compared with that of As_2Se_3 ($=3 \times 10^{-13}\ \Omega^{-1}\ \mathrm{cm}^{-1}$) [36], where the SRO in As_2Se_3 is chemically ordered involving only As–Se bonds and the satisfied 8-N rule.

5. Conclusion

A new method, based on using an electronic distribution function $\sigma(r)$ without a sharpening factor, was used for scaling the corrected x-ray scattered intensity. The present results of the scattered x-ray intensity stated that the weak medium-range order (MRO) in the glassy As_2Te_3 is owing to the high metallic nature of the bonds. Gaussian fitting of the first peak on the total radial distribution function added a new evidence that the short-range order of the As_2Te_3 glassy sample is different from that in the crystalline state and that the arrangements of the atoms in the first coordination sphere is chemically disordered, i.e. As–As and Te–Te bonds, in addition to the As–Te bonds, are found.

Table 2. Comparison of the first-order atomic distances, r_{n-m}, root-mean-square displacement, $\langle u^2_{n-m}\rangle$, partial coordination number, N_{n-m}, total coordination number N_i, derived from x-ray (method 1) and EXAFS (method 2) for glassy As_2Te_3.

		As–As			As–Te			Te–Te			As	Te
Met.	Reference	r (Å)	$\langle u^2\rangle$ (Å^2)	N	r (Å)	$\langle u^2\rangle$ (Å^2)	N	r (Å)	$\langle u^2\rangle$ (Å^2)	N	N	N
1	[1]	—	—	0	2.6	—	3.0	—	—	0	3.0	2.00
1	[2]	—	—	0	2.66	—	3.0	—	—	—	3.0	2.00
1	[34]	2.47	—	0.80	2.69	—	2.1	2.83	—	1.1	—	—
1	This work	2.50 ± 0.003	0.050	0.85 ± 0.02	2.7 ± 0.01	0.064	2.1 ± 0.03	2.8 ± 0.03	0.075	0.93 ± 0.03	2.95 ± 0.04	2.33 ± 0.03
2	[5]	2.47	—	0.80	2.66	—	2.2	2.80	—	0.90	3.0	2.40

References

[1] Fitzpatrick J R and Maghrabi C 1971 *Phys. Chem. Glasses* **12** 105
[2] Cornet J and Rossier D 1973 *J. Non-Cryst. Solids* **12** 85
[3] Vasil L N, Kryl'nikov Yu V, Kamolov A K and Sergein P P 1976 *Akad. Nauk USSR, Neorg. Matter.* **12** 350
[4] Červinka L and Hrubý A 1982 *J. Non-Cryst. Solids* **48** 231
[5] Ma Q, Raoux D and Benzetch S 1993 *Phys. Rev.* B **48** 16332
[6] Tverjanovich A, Yagodkina M and Strykanov V 1998 *J. Non-Cryst. Solids* **223** 86
[7] Himmel B, Gerber Th, Heyer H and Blau W 1987 *J. Mater. Sci.* **22** 1374
[8] Klug H P and Alexander L E 1974 *X-ray Diffraction Procedures for Polycrystalline and Amorphous Materials* (New York: Wiley)
[9] Hajdu F and Palinkas G 1972 *J. Appl. Crystallogr.* **5** 395
[10] *International Tables for X-ray Crystallography* 1974 vol IV (Birmingham: Knoch Press)
[11] Wagner C N J 1969 *J. Vac. Sci. Technol.* **6** 650
[12] Krogh–Moe J 1956 *Acta. Crystallogr.* **9** 951
[13] Elliot S R 1983 *Physics of Amorphous Materials* Longman Group limited p 66
[14] Cargill G S 1970 *J. Appl. Phys.* **41** 12
[15] Habenschuss A and Spedding F H 1979 *J. Chem. Phys.* **70** 2797
[16] Stetsiv Ya I 1973 *Sov. Phys.—Crystallogr.* **18** 158
[17] Erenburg A, Gartstein E and Landau M 2005 *J. Phys. Chem. Solids* **66** 81
[18] Himmel B, Gerber Th, Heyer W and Blau W 1987 *J. Mater. Sci.* **22** 1374
[19] Uemura O, Usuki T, Inoue M, Abe K, Kameda Y and Sakurai M 2001 *J. Non-Cryst. Solids* **293–295** 792
[20] Sharma D, Sampath S, Lalla N P and Awasthi A M 2005 *Physica* B **357** 290
[21] Zarzycki J 1991 *Glasses and the Vitrous State* (Cambridge: Cambridge University Press) p 89
[22] Grigorovici R 1974 *Amorphous and Liquid Semiconductors* ed J Tauc (New York: Plenum) p 45
[23] Susman S, Volin K J, Montague D G and Price D L 1990 *J. Non-Cryst. Solids* **125** 168
[24] Lee J H, Owens A P, Pradel A, Hannon A C, Ribes M and Elliot S R 1996 *Phys. Rev.* B **54** 3895
[25] Mamedov S, Bolotov A, Brinker L, Kisliuk A and Soltwitsh A 1998 *J. Non-Cryst. Solids* **224** 89
[26] Vaipolin A A and Pori-koshits E A 1974 *Sov. Phys.—Solid State* **15** 250
[27] Mori T, Yasuoka H, Saugusa H, Okawa K, Kato M, Arai T, Fikunaga T and Watanabe N 1983 *Japan J. Appl. Phys.* **22** 1784
[28] Tanaka K 1998 *Japan J. Appl. Phys.* **37** 1747
[29] Carron J 1963 *Acta Crystallogr.* **16** 338
[30] Uemura O, Sagar Y, Tsushima M, Kamikawa T and Satow T 1979 *J. Non-Cryst. Solids* **33** 71
[31] Ramesh Rao N, Karishna P S R, Basu S, Dasannacharya B A, Sangunni K S and Gopal E S R 1998 *J. Non-Cryst. Solids* **240** 221
[32] Mott N F 1967 *Adv. Phys.* **16** 49
[33] Chang J and Dove D B 1974 *J. Non-Cryst. Solids* **16** 72
[34] Kameda Y, Usuki T and Uemura O 1996 *J. Non-Cryst. Solids* **205–207** 130
[35] Usuki T, Itoh K, Kameda Y and Uemura O 1998 *Mater. Trans., JIM* **39** 1135
[36] Feltz A 1993 *Amorphous Inorganic Materials and Glasses* (New York: VCH Verlagsgesellschaft) p 209